

- (32) Ledford, E. B., Jr.; White, R. L.; Gadheri, S.; Wilkins, C. L.; Gross, M. L. *Anal. Chem.* **1980**, *52*, 2450-2451.
- (33) Pine, S. H.; Hendrickson, J. B.; Cram, D. S.; Hammond, J. S. *Organic Chemistry*; McGraw-Hill International Book Co.: Tokyo, 1980; p 285.
- (34) Lund, H. *Acta Chim. Scand.* **1959**, *13*, 249-267.
- (35) Cooks, R. G.; Varvoglis, A. G. *Org. Mass Spectrom.* **1971**, *5*, 687-696.
- (36) Leyshon, W. M.; Wilson, D. A. *Org. Mass Spectrom.* **1973**, *7*, 251-257.
- (37) Thorstad, O.; Undheim, K.; El-Gendy, M. A. F. *Org. Mass Spectrom.* **1975**, *10*, 1155-1159.
- (38) Vijfhuizen, P. C.; Heerma, W.; Dijkstra, G. *Org. Mass Spectrom.* **1975**, *10*, 919-929.
- (39) Vijfhuizen, P. C.; Terlow, J. K. *Org. Mass Spectrom.* **1977**, *12*, 245-253.
- (40) Kallury, R. K. M. R.; Rao, P. L. K. M. *Org. Mass Spectrom.* **1977**, *12*, 411-415.
- (41) Lachman, A. *Organic Synthesis, Collective Volume II*; Wiley: New York, 1943; pp 234-236.
- (42) Deem, M. L. *Org. Mass Spectrom.* **1980**, *15*, 573-577.
- (43) Busch, K. L.; Cooks, R. G. *Science* **1982**, *218*, 247-254.
- (44) Vincze, A.; Busch, K. L.; Cooks, R. G. *Anal. Chim. Acta* **1982**, *136*, 143-153.
- (45) De Pauw, E. *Mass Spectrom. Rev.* **1986**, *5*, 191-212.
- (46) Day, R. J.; Unger, S. E.; Cooks, R. G. *Anal. Chem.* **1980**, *52*, 557A-572A.
- (47) De Pauw, E.; Pelzer, G.; Marien, J.; Piette, J. L.; Pardon, M. C. *Org. Mass Spectrom.* **1985**, *20*, 692-693.
- (48) Ligon, W. V., Jr. *Anal. Chem.* **1986**, *58*, 487-490.
- (49) Ligon, W. V., Jr.; Dorn, S. B. *Int. J. Mass Spectrom. Ion Processes* **1985**, *63*, 315-324.
- (50) Gardner, H. J.; Georgans, W. P. *J. Chem. Soc.* **1956**, 4180-4186.

RECEIVED for review September 13, 1988. Accepted March 15, 1989. The authors are indebted to the INIC (Instituto Nacional de Investigacao Científica) for a scholarship given to M. G. Santana-Marques. This work was supported in part by the Midwest Center for Mass Spectrometry, a National Science Foundation facility (Grant No. CHE 8620177).

# Ion Confinement in the Collision Cell of a Multiquadrupole Mass Spectrometer: Access to Chemical Equilibrium and Determination of Kinetic and Thermodynamic Parameters of an Ion-Molecule Reaction

Claude Beaugrand

*SN Nermag, 49 quai du Halage, 92500 Rueil-Malmaison, France*

Daniel Jaouen, Hélène Mestdagh, and Christian Rolando\*

*Ecole Normale Supérieure, Département de Chimie, Laboratoire de l'Activation Moléculaire, UA 1110, 24 rue Lhomond, 7531 Paris Cedex 05, France*

**Ions can be confined in an rf-only collision cell of a tandem quadrupole mass spectrometer so that ion-molecule reactions can be studied for variable interaction times (0.05-250 ms). The chemical system studied (ammonium ion, pyrrolidine, piperidine) involved the following reactions: proton exchange, formation of proton-bound dimers, and amine exchange between dimers. Chemical equilibrium could be reached for the exchange reactions. The equilibrium constants of these reactions, as well as the rate constants of the different reactions involved, were thus easily determined from the variation of relative abundance of reactant and product ions versus confinement time.**

Detailed kinetic and thermodynamic data concerning ion-molecule reactions are useful both from a fundamental point of view and as a basis for designing analytical uses of these reactions for mass spectrometry. The most direct way of obtaining such information is to provide for a variable reaction time under a given set of conditions and to observe the variation of reactant and product ion abundances. Numerous such experiments have been performed either in ICR (ion cyclotron resonance) cells (1) (reaction pressure:  $10^{-8}$  to  $10^{-5}$  Torr) or in high-pressure ion sources (see for example ref 2-5) and flow tube instruments (6) (reaction pressure: a few Torr). It is interesting to make this possibility available in the rf-only collision cell of a quadrupole spectrometer, which allows investigations in an intermediate pressure range ( $10^{-5}$  to  $10^{-2}$  Torr). Quadrupole ion traps (reaction pressure:  $10^{-7}$  to  $10^{-4}$

Torr) have also been used in this way (7, 8).

Thus, we modified the operation of a rf-only collision cell of our multiquadrupole MS/MS/MS instrument in order to control the duration of an ion-molecule reaction, i.e., to trap ions in the cell for a variable time. A similar trapping device has been used to improve the efficiency of reaction product detection in a MS/MS quadrupole spectrometer (9). Providing the interaction time is long enough, one can expect to reach chemical equilibrium for a reversible reaction and thus determine its equilibrium constant.

The ion confinement technique was first tested on a simple process: collisionally activated dissociation of the  $\text{FeCO}^+$  ion leading to the  $\text{Fe}^+$  fragment ion (10). We now wish to report its application to the study of ion-molecule reactions, showing that chemical equilibrium actually can be attained under ion confinement conditions.

In order to determine the efficiency of this method, we chose to confine  $\text{NH}_4^+$  ions with a mixture of pyrrolidine and piperidine in the collision cell. The reactions involved are proton exchanges and formation of proton-bound dimers. This system seemed suitable for our purpose because (i) it is of reasonable complexity, having six different ions present in the reaction mixture; and (ii) such reactions were studied under ICR conditions, so that some of the kinetic and thermodynamic data obtained can be compared with literature values.

## EXPERIMENTAL SECTION

The experiments were performed on a prototype MS/MS/MS multiquadrupole mass spectrometer described elsewhere (11). Briefly, it is composed of the following parts: source (electron

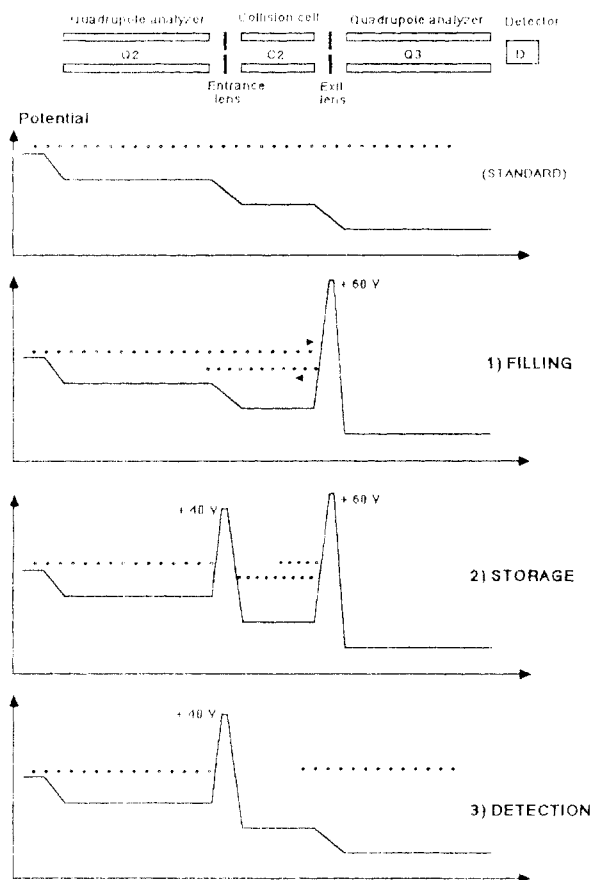


Figure 1. Successive stages of a confinement cycle.

impact, chemical ionization, or fast atom bombardment), first quadrupole analyzer, first rf-only collision cell, second analyzer, second rf-only collision cell, third analyzer, and detector. In all the experiments described here, the first collision cell contained no collision gas, and the second analyzer was left in the rf-only mode. Ion confinement was performed in the second collision cell, using the entrance and exit lenses of this cell as electrostatic mirrors. The potentials of the lenses were varied according to the confinement cycle described below. The corresponding potentials were generated by a two-channel fast rise power supply driven by an auxiliary microcomputer slave of the main data system. The power supply from SN Nermag has the following characteristics: continuously adjustable output voltage 0–100 V, input voltage 0–5 V; the maximum frequency allowed without distortion of the signal is 50 kHz. The auxiliary data system is a personal computer with a homemade 8-bit digital-to-analog interface. The confinement cycle is defined by the following parameters: filling time, storage time, and detection time. The minimum value allowed by the system for one operation is 50  $\mu$ s. EMMA, the main data acquisition system, was modified so as to trigger the confinement cycle. This improvement allows one to record standard mass spectra in the confinement mode.

Ammonium ions were generated in the source by chemical ionization using ammonia. Piperidine and pyrrolidine were purified by distillation over calcium hydride. Equal weights of liquid piperidine and pyrrolidine were mixed in a flask connected to the cell via a controlled leak valve from Riber Co. (Rueil-Malmaison, France). The composition of the gas mixture was determined by  $^1\text{H}$  and  $^{13}\text{C}$  NMR after pumping a small amount of vapor over the liquid mixture and condensing it into a cold trap: The measured pyrrolidine to piperidine molar ratio was  $1.9 \pm 0.1$ . The absolute pressure in the collision cell was measured by using a Bayard-Alpert gauge, calibrated for the mixture to be studied with a capacitance manometer from MKS Instruments, Inc. (Andover, MA).

## RESULTS AND DISCUSSION

**The Confinement Cycle.** The entrance and exit lenses of the collision cell were used as cell doors. At its normal low

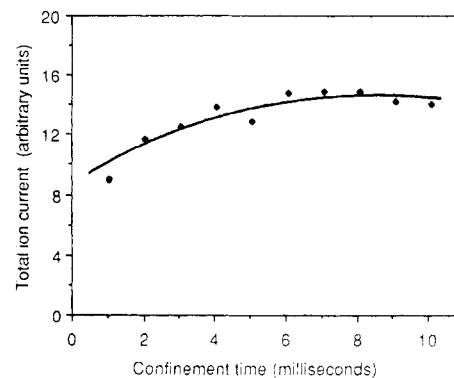


Figure 2. Variation of total ion current with confinement time in a given series of experiments.

potential, a lens allows the ions through (open door), whereas at high potential it functions as an electrostatic mirror (closed door). Figure 1 displays the potentials applied to the lenses during the following successive stages of a confinement cycle: (1) *Filling Stage* (250  $\mu$ s). The entrance lens is at its normal low potential, and the exit lens is at a high potential, i.e., 2 or 3 times the average kinetic energy of the incoming ions.

(2) *Storage Stage* (Variable Time). Both lenses are at high potential.

(3) *Detection Stage* (250  $\mu$ s). The exit lens is switched to low potential, while the entrance lens is kept at high potential; ions are thus allowed to reach the last analyzer.

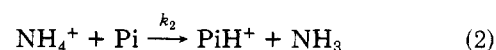
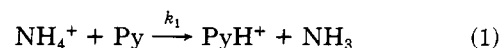
The entire cycle is then repeated after a delay time.

The confinement time can be varied from a few hundredths of a millisecond to 250 ms. In order to scan a range of confinement time in a single experiment, the time can be automatically increased by a defined step. Figure 2 shows that in such an experiment the total ion current measured remained fairly independent of the confinement time. This means that little ion loss occurred during the storage step, showing the high efficiency of the confinement device.

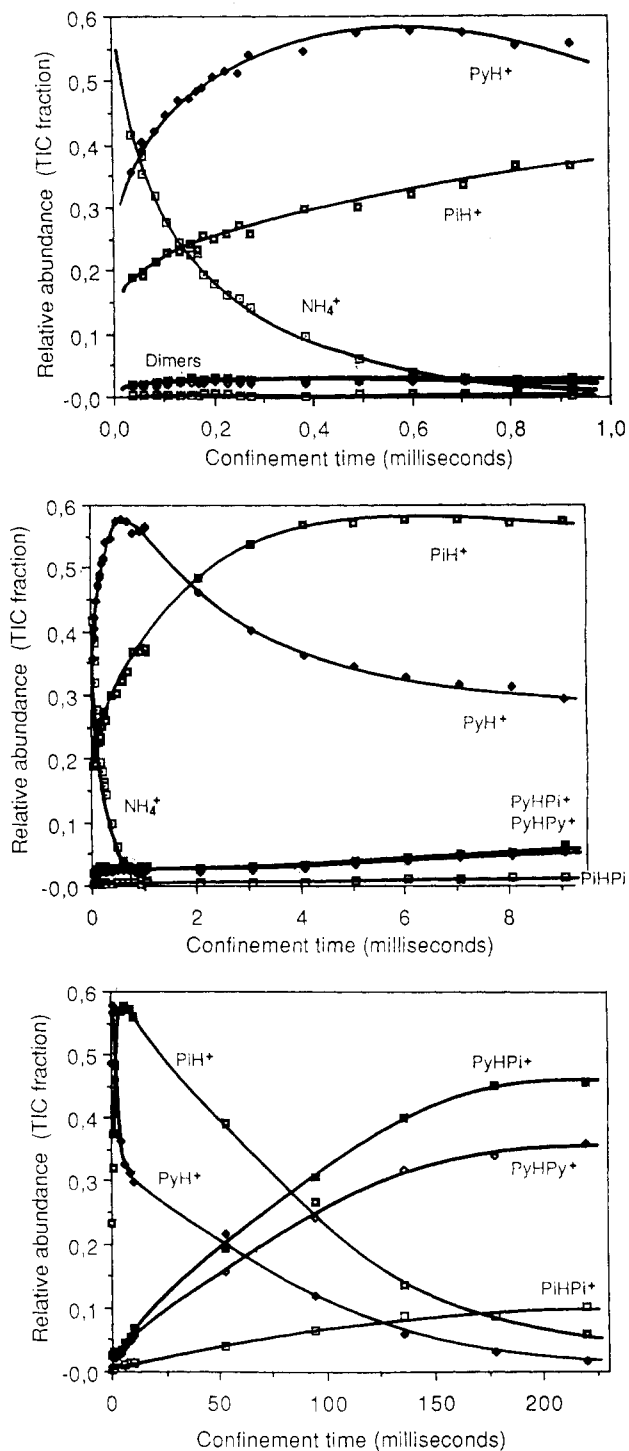
**Variation of Relative Abundances of Reagent and Product Ions versus Confinement Time.** The reaction of ammonium ions with the pyrrolidine–piperidine mixture was followed at five different pressures ( $1.0 \times 10^{-5}$  to  $2.7 \times 10^{-4}$  Torr), with the confinement time varying from 0.035 to 10.1 ms. For one pressure ( $5.3 \times 10^{-5}$  Torr) the confinement time was increased up to 220 ms. The reaction mixtures consisted of the following six ions in variable proportions according to the different reaction periods:  $\text{NH}_4^+$  ( $m/z$  18), reagent ion;  $\text{C}_4\text{H}_{10}\text{N}^+$  ( $m/z$  72), protonated pyrrolidine ( $\text{PyH}^+$ );  $\text{C}_5\text{H}_{12}\text{N}^+$  ( $m/z$  86), protonated piperidine ( $\text{PiH}^+$ );  $\text{C}_8\text{H}_{19}\text{N}_2^+$  ( $m/z$  143), pyrrolidine proton-bound dimer ( $\text{PyHPy}^+$ );  $\text{C}_9\text{H}_{21}\text{N}_2^+$  ( $m/z$  157), pyrrolidine–piperidine proton-bound mixed dimer ( $\text{PyHPi}^+$ );  $\text{C}_{10}\text{H}_{23}\text{N}_2^+$  ( $m/z$  171), piperidine proton-bound dimer ( $\text{PiHPi}^+$ ).

Figure 3 displays the variation of the relative abundance of each of these ions with confinement time at a  $5.3 \times 10^{-5}$  Torr pressure. The pattern of these abundance curves allows qualitative analysis of the successive processes occurring in the reaction mixture.

(i) 0–1 ms.  $\text{NH}_4^+$  decreases to 0;  $\text{PyH}^+$  and  $\text{PiH}^+$  increase because the initial reaction is protonation of the amines by  $\text{NH}_4^+$  ions.

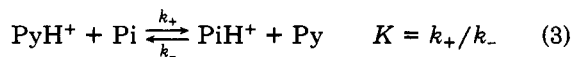


The relative amounts of  $\text{PyH}^+$  versus  $\text{PiH}^+$  formed by these reactions are kinetically controlled, so that the mixture initially formed is not in equilibrium.



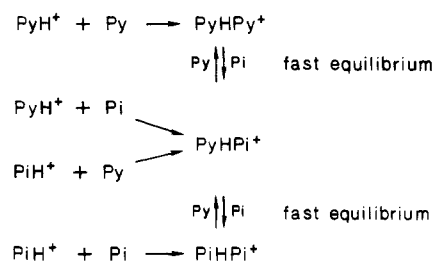
**Figure 3.** Variation of relative abundance of reactant and product ions with confinement time at a 0.053-mTorr pressure, for short (a, top), medium (b, middle), and long (c, bottom) confinement times.

(ii) 1–10 ms.  $\text{PyH}^+$  decreases,  $\text{PiH}^+$  increases; the dominant reaction is proton exchange leading to the acid–base equilibrium



(iii) 1–220 ms. Concurrently with the preceding reaction and throughout the confinement period, a slow increase of dimer abundance ( $\text{PyHPy}^+$ ,  $\text{PyHPi}^+$ ,  $\text{PiHPi}^+$ ) is observed. However, their abundance ratios relative to each other rapidly become independent of time (see Figures 5 and 6 for the corresponding curves), showing that equilibrium is achieved among the dimers. This means that the dimers undergo amine exchange much faster than they are formed from their mo-

nomer precursors, according to the following scheme:



The abundance curves obtained at other pressures display similar features. As expected, all the reaction rates increased with pressure. For the lowest pressure used ( $1.0 \times 10^{-5}$  Torr) no significant amount of dimers had yet formed after 10 ms, and chemical equilibrium for reaction 3 had not yet been attained.

These results are entirely consistent with the ICR studies of amine protonation and dimerization; the shapes of the curves obtained are similar to those reported for protonation and dimerization of an azetidine–pyrrolidine mixture (12).

In the experiments performed, the dimer abundance had not reached a constant value for the longest (220 ms) confinement time studied, indicating that thermodynamic equilibrium had not been attained with regard to dimerization reactions. Our results indicate, however, that this equilibrium is shifted far toward dimerization, since in two cases ( $P = 5.3 \times 10^{-5}$  Torr, confinement up to 220 ms, and  $P = 2.7 \times 10^{-4}$  Torr, confinement up to 10 ms) dimers constituted, respectively, more than 92% and 96% of the final reaction mixture. The temperature dependence of the equilibrium constant of pyrrolidine dimerization was recently determined (13). Extrapolation to room temperature of the corresponding linear plot of  $\ln K$  versus  $1/T$  leads to an approximate  $K$  value of  $10^8 \text{ Torr}^{-1}$ , which means that within the pressure range used in our experiment ( $10^{-5}$  to  $10^{-3}$  Torr) the remaining monomers would not be detectable if the equilibrium were completely achieved.

No significant amount of trimer was detected in our experiments. A minor amount of pyrrolidine trimer (ca. 10% at  $10^{-4}$  Torr) should be present, however, at equilibrium (13). The trimerization reaction is likely far too slow to be detected under the conditions used.

These results illustrate the utility of ion confinement in characterizing the successive steps of a chemical process in the gas phase. Furthermore, knowledge of the relative concentrations of reactant and product ions as a function of reaction (confinement) time allows one to obtain quantitative thermodynamic and kinetic data concerning the reactions involved.

**Determination of Equilibrium Constants. Proton Exchange between Piperidine and Pyrrolidine (Reaction 3).** Figure 4 shows the variation of the  $\text{PiH}^+/\text{PyH}^+$  ratio with confinement time. Except at the lowest pressure, this ratio clearly attains a constant equilibrium value, independent of pressure:  $(\text{PiH}^+/\text{PyH}^+)_e = 1.85 \pm 0.15$ .

The equilibrium constant of reaction 3 thus can be determined:

$$K = (\text{PiH}^+/\text{PyH}^+)(\text{Py}/\text{Pi}) = 3.5$$

$$\text{corresponding to } \Delta G^\circ = -3.1 \text{ kJ mol}^{-1} = -0.74 \pm 0.10 \text{ kcal mol}^{-1}$$

Although slightly lower than those determined by other workers, this value is in agreement with them within experimental uncertainties:

$$\Delta G^\circ = \text{GB}(\text{Py}) - \text{GB}(\text{Pi}) = -1.1 \pm 0.2 \text{ kcal mol}^{-1} \quad (14)$$

$$= -0.9 \text{ kcal mol}^{-1} \quad (15)$$

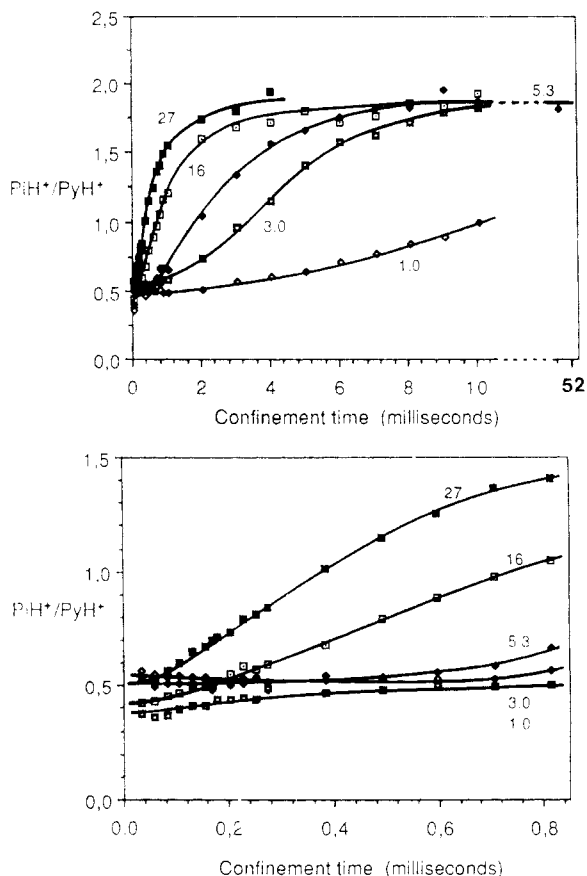


**Figure 4.** Variation of the  $\text{PiH}^+/\text{PyH}^+$  ratio with confinement time for the different pressures used (pressures indicated in  $10^{-5}$  Torr units): medium (a, top) and short (b, bottom) confinement times.

where  $\text{GB}(\text{Pi})$  and  $\text{GB}(\text{Py})$  are the gas-phase basicities of piperidine and pyrrolidine, relative to the same absolute scale.

It was pointed out by Bowers et al. that competitive dimerization may alter the measurement of proton-exchange equilibrium constants, the apparent equilibrium being shifted toward the more slowly dimerizing species (16). Because of the fast amine exchange between the three dimers, individual dimerization rates are not accessible from our experiments. However, comparison between the average dimerization rate and the proton-exchange rate (see below for determination of the corresponding rate constants) shows that even if one amine dimerizes much faster than the other, no significant error is introduced in the  $K$  value for the pressure range studied. This is supported by the fact that  $K$  is pressure-independent within experimental uncertainties.

**Base Exchange between Dimers.** These reactions correspond to eq 4 and 5:



Figures 5 and 6 show the variation of  $\text{PyHPi}^+/\text{PyHPy}^+$  and  $\text{PiHPi}^+/\text{PyHPi}^+$  ratios, respectively, with confinement time. Both of these ratios attain their equilibrium value at the four pressures used:

$$(\text{PyHPi}^+/\text{PyHPy}^+)_e = 1.2 \pm 0.2$$

$$(\text{PiHPi}^+/\text{PyHPi}^+)_e = 0.20 \pm 0.04$$

The dispersion of the results is slightly larger than in the preceding case, probably because in these experiments dimers

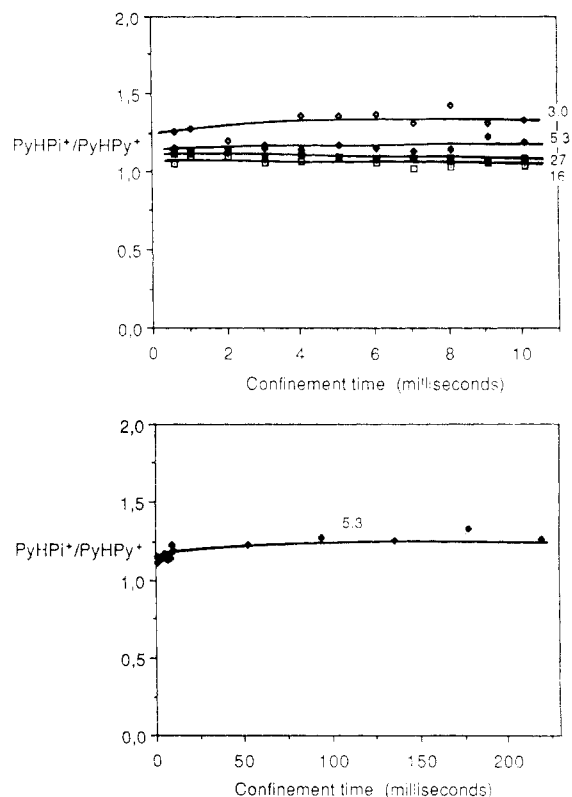


**Figure 5.** Variation of the  $\text{PyHPi}^+/\text{PyHPy}^+$  ratio with confinement time for the different pressures used (pressures indicated in  $10^{-5}$  Torr units): medium (a, top) and long (b, bottom) confinement times.

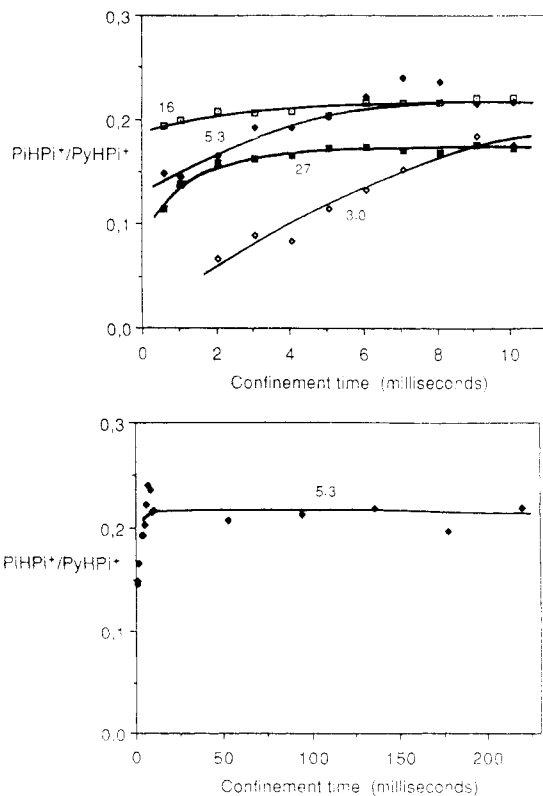


**Figure 6.** Variation of the  $\text{PiHPi}^+/\text{PyHPi}^+$  ratio with confinement time for the different pressures used (pressures indicated in  $10^{-5}$  Torr units): medium (a, top) and long (b, bottom) confinement times.

are very often minor components of the reaction mixture. These ratios lead to the following equilibrium constants:

$$K_4 = (\text{PyHPi}^+/\text{PyHPy}^+)_e (\text{Py}/\text{Pi}) = 2.3$$

corresponding to  $\Delta G^\circ_4 = -2.0 \text{ kJ mol}^{-1} =$   
 $-0.48 \pm 0.15 \text{ kcal mol}^{-1}$

$$K_5 = (\text{PiHPi}^+/\text{PyHPi}^+)_e(\text{Py}/\text{Pi}) = 0.38$$

corresponding to  $\Delta G^\circ_5 = 2.4 \text{ kJ mol}^{-1} =$   
 $0.56 \pm 0.20 \text{ kcal mol}^{-1}$

These values are close to those that can be calculated from reported molecule pair gas-phase basicities (MPGB) (17):

$$\Delta G^\circ_4 = \text{MPGB}(\text{PyHPy}^+) - \text{MPGB}(\text{PyHPi}^+) =$$

$$-0.5 \text{ kcal mol}^{-1}$$

$$\Delta G^\circ_5 = \text{MPGB}(\text{PyHPi}^+) - \text{MPGB}(\text{PiHPi}^+) =$$

$$0.2 \text{ kcal mol}^{-1}$$

The formation of a proton-bound dimer from an acid  $\text{AH}^+$  and a base B was shown to be increasingly exoenergetic with increasing acidity of  $\text{AH}^+$  and with increasing basicity of B (18, 19). Consider the dimerization equilibria



As piperidine is more basic than pyrrolidine, these free energies should verify the following relationships:

$$\Delta G^\circ(\text{PyPi}) < \Delta G^\circ(\text{PyPy}) < \Delta G^\circ(\text{PiPy})$$

$$\Delta G^\circ(\text{PyPi}) < \Delta G^\circ(\text{PiPi}) < \Delta G^\circ(\text{PiPy})$$

The preceding free energies are related to the experimental free energies  $\Delta G^\circ$ ,  $\Delta G^\circ_4$ , and  $\Delta G^\circ_5$ :

$$\Delta G^\circ(\text{PyPi}) - \Delta G^\circ(\text{PyPy}) = \Delta G^\circ_4 = -0.5 \text{ kcal/mol}$$

$$\Delta G^\circ(\text{PyPy}) - \Delta G^\circ(\text{PiPy}) = \Delta G^\circ - \Delta G^\circ_4 =$$

$$-0.3 \text{ kcal/mol}$$

$$\Delta G^\circ(\text{PyPi}) - \Delta G^\circ(\text{PiPi}) = \Delta G^\circ - \Delta G^\circ_5 =$$

$$-1.3 \text{ kcal/mol}$$

$$\Delta G^\circ(\text{PiPi}) - \Delta G^\circ(\text{PiPy}) = \Delta G^\circ_5 = +0.6 \text{ kcal/mol}$$

The expected inequalities are therefore verified, with the exception of the last one. This may be interpreted as  $\Delta G^\circ(\text{PiPi})$  being slightly higher than expected, possibly because of steric interactions hindering piperidine dimerization more than formation of the other two proton-bound dimers. Since the basicities of piperidine and pyrrolidine are close to each other, even a slight steric effect may reverse the order of the free energy values under consideration.

**Reaction Temperature.** In the preceding considerations we have assumed a reaction temperature of 298 K, i.e. the temperature of the collision gas in the cell. However, the reacting ions may not be thermalized at this temperature, since their average translational energy may be modified by the variable electric field present in the collision cell. In order to check the validity of our initial assumption concerning temperature (this point was raised by a reviewer) two experiments were performed:

(i) Variation of the rf power of the cell quadrupole. The position of the piperidine-pyrrolidine proton-exchange equilibrium was observed to be insensitive to this variation.

(ii) Study of a known temperature-dependent equilibrium. Proton exchange between triethylamine and putrescine (20) was chosen for this purpose. Ammonium ions were reacted with mixtures of triethylamine and putrescine in the collision cell until the protonated triethylamine to protonated putrescine ratio attained its equilibrium value. In this experiment the collision cell was slightly heated (ca. 50 °C) due to the low volatility of putrescine. The equilibrium ratio,

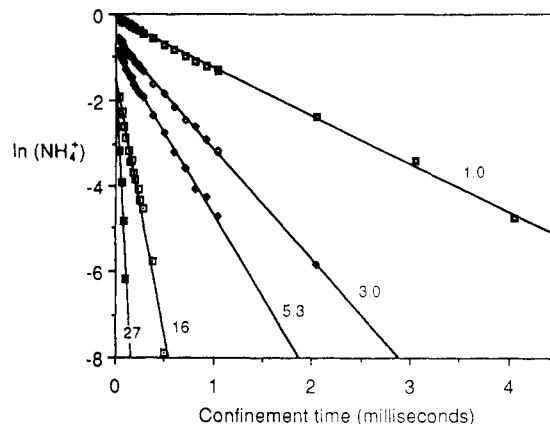


Figure 7. Variation of  $\ln(\text{NH}_4^+)$  with confinement time for the different pressures used (pressures indicated in  $10^{-5}$  Torr units).

joined to the pressure ratio of the two amines, allowed us to determine the corresponding equilibrium constant:  $1.16 \pm 0.1$ . According to the temperature dependence reported in ref 20, this corresponded to a temperature of 330 K, in fair agreement with the temperature of the gas in the cell. These measurements were performed at a total pressure of  $10^{-5}$  to  $10^{-4}$  Torr, i.e. in the same pressure range as with the pyrrolidine-piperidine mixture. However, experiments done in a wider pressure range on trimethylamine proton-bound dimer formation equilibrium (18) have shown that at the highest pressures usable in the cell (a few milliTorr) the apparent reaction temperature is much higher than the gas temperature. These phenomena are under investigation.

**Determination of Rate Constants.** *Amine Protonation by Ammonium Ion (Reactions 1 and 2).* Figure 7 shows the variation of  $\ln(\text{NH}_4^+)$  versus confinement time for the different pressures used. The corresponding curves are linear, in agreement with the expected rate law:

$$d(\text{NH}_4^+)/dt = [k_1(\text{Py}) + k_2(\text{Pi})](\text{NH}_4^+)$$

$$\ln(\text{NH}_4^+) = -[k_1(\text{Py}) + k_2(\text{Pi})]t = -k_p t$$

With  $a = (\text{Py})/(\text{Pi}) = 1.9$  and  $P = \text{total pressure}$

$$k_p = P(k_1 + k_2 a)/(1 + a)$$

Plotting  $k_p$  values (slopes of the different curves of Figure 7) versus pressure  $P$  showed that  $k_p$  is actually proportional to  $P$ . The corresponding slope is

$$k_p^\circ = 2.22 \times 10^{-9} \text{ s}^{-1} \text{ molecule}^{-1} \text{ cm}^3 =$$

$$(k_1 + k_2 a)/(1 + a)$$

The second relationship needed to determine  $k_1$  and  $k_2$  is obtained by evaluating the  $k_1/k_2$  ratio: For short reaction times the  $(\text{PiH}^+)/(\text{PyH}^+)$  ratio should tend to be constant and equal to  $k_2(\text{Pi})/k_1(\text{Py})$ , since reaction 3 is much slower than reactions 1 and 2. Figure 4b shows that this is actually the case (as expected it is more apparent at the lowest pressures) and allows one to determine  $k_2/k_1$ :

$$k_2(\text{Pi})/k_1(\text{Py}) = [(\text{PiH}^+)/(\text{PyH}^+)]_0 = 0.48 \pm 0.1$$

$$k_2/k_1 = a[(\text{PiH}^+)/(\text{PyH}^+)]_0 = 0.91 \pm 0.25$$

The rate constants  $k_1$  and  $k_2$  are then derived from the values of  $k_p^\circ$  and  $k_2/k_1$ :

$$k_1 = (2.3 \pm 0.5) \times 10^{-9} \text{ s}^{-1} \text{ molecule}^{-1} \text{ cm}^3$$

$$k_2 = (2.1 \pm 0.5) \times 10^{-9} \text{ s}^{-1} \text{ molecule}^{-1} \text{ cm}^3$$

The values of  $k_1$  and  $k_2$  are close to each other, which is not surprising as piperidine and pyrrolidine are approximately the same size and are both much more basic than ammonia, so their proton-transfer cross sections with the ammonium

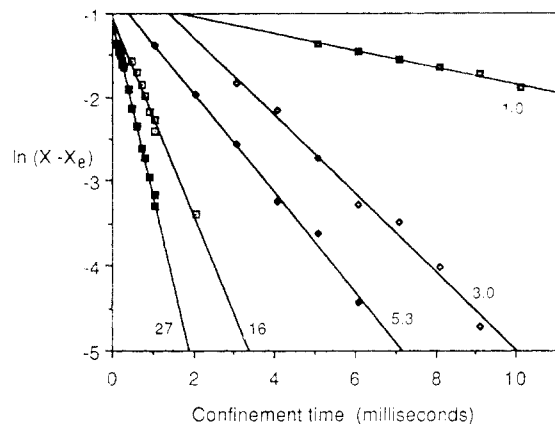


**Figure 8.** Variation of  $\ln(X - X_e)$  (see text for definition) with confinement time for the different pressures used (pressures indicated in  $10^{-5}$  Torr units).

ion have no reason to be very different. These rate constants are also of the same order of magnitude as those reported for protonation of piperidine and pyrrolidine by their respective radical cations (21). They are in good agreement with the values calculated from the ADO theory of Su and Bowers (22):  $2.60 \times 10^{-9} \text{ s}^{-1} \text{ molecule}^{-1} \text{ cm}^3$  for pyrrolidine and  $2.46 \times 10^{-9} \text{ s}^{-1} \text{ molecule}^{-1} \text{ cm}^3$  for piperidine.

*Proton Exchange between Pyrrolidine and Piperidine (Reaction 3).* Determination of the corresponding rate constants  $k_+$  and  $k_-$  can be done after complete disappearance of ammonium ions, i.e. excluding short reaction times. As will be shown below, dimerization reactions are much slower than proton exchange (the largest  $k_d/k_e$  ratio, corresponding to the highest pressure used, is  $0.23 \text{ ms}^{-1}/2.1 \text{ ms}^{-1} = 0.11$ ). Thus it can be assumed that concurrent dimerization reactions have negligible rates versus proton-exchange rates. The following rate law can then be expected:

$$d(X - X_e)/dt = -[k_+(\text{Pi}) + k_-(\text{Py})](X - X_e)$$

where  $X = (\text{PiH}^+)/[(\text{PiH}^+) + (\text{PyH}^+)]$  and  $X_e$  is the equilibrium value of  $X$ .

$$\begin{aligned} \ln(X - X_e) &= \ln(X_0 - X_e) - [k_+(\text{Pi}) + k_-(\text{Py})]t \\ &= \ln(X_0 - X_e) - k_e t \end{aligned}$$

$$k_e = P(k_- + k_+a)/(1 + a) = k_e^\circ P$$

Figure 8 displays  $\ln(X - X_e)$  versus confinement time, showing that the corresponding curves are linear. Their slopes  $k_e$  were plotted versus pressure  $P$ . The slope of the resulting linear curve is

$$k_e^\circ = 7.0 \text{ ms}^{-1} \text{ mTorr}^{-1} = 2.14 \times 10^{-10} \text{ s}^{-1} \text{ molecule}^{-1} \text{ cm}^3$$

$k_+$  and  $k_-$  are then easily determined, since  $k_+/k_- = K = 3.5$ .

$$k_+ = (2.8 \pm 0.5) \times 10^{-10} \text{ s}^{-1} \text{ molecule}^{-1} \text{ cm}^3$$

$$k_- = (8.1 \pm 2) \times 10^{-11} \text{ s}^{-1} \text{ molecule}^{-1} \text{ cm}^3$$

*Dimerization Reactions.* As already pointed out, these experiments do not give access to the individual dimerization rate constants, because of fast equilibration occurring among the dimers. An average dimerization rate constant  $k_d$  can be defined as follows:

$$d[(\text{PyHPy}^+) + (\text{PyHPi}^+) + (\text{PiHPi}^+)]/dt = k_d[(\text{PyH}^+) + (\text{PiH}^+)]$$

As in the preceding case we consider only reaction times long enough so that no ammonium ion is present in the reaction mixture. With  $S = (\text{PyH}^+) + (\text{PiH}^+)$

$$d(1 - S)/dt = k_d S$$

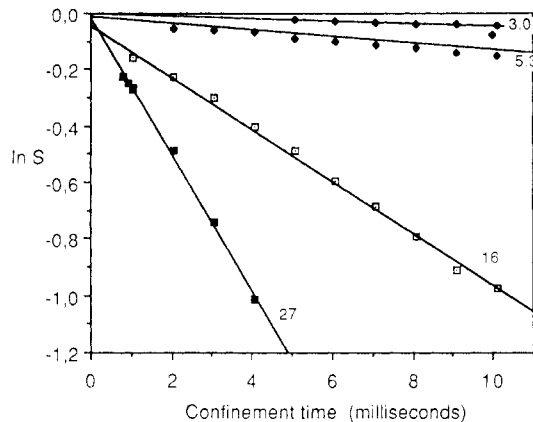


**Figure 9.** Variation of  $\ln S = \ln[(\text{PyH}^+) + (\text{PiH}^+)]$  with confinement time for the different pressures used (pressures indicated in  $10^{-5}$  Torr units), for medium confinement times. The points obtained for longer confinement times (up to 220 ms) at  $5.3 \times 10^{-5}$  Torr pressure are aligned with those shown here and are included in the represented linear regression.

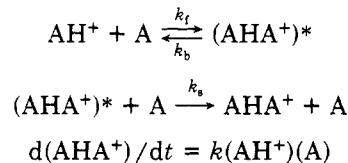
$k_d$  will remain constant with reaction time providing equilibrium 3 is achieved, or if the individual dimerization rate constants have similar values. In that case we expect the following relationship:

$$\ln S = \ln S_0 - k_d t$$

Figure 9 displays  $\ln S$  versus confinement time for the different pressures used, showing that the corresponding curves are linear. Their slopes,  $k_d$ , when plotted versus  $P$  and versus  $P^2$ , appeared to be proportional to  $P^2$ :  $k_d = k_d^\circ P^2$ .

$$k_d^\circ = 3.3 \text{ ms}^{-1} \text{ mTorr}^{-2} = 3.0 \times 10^{-24} \text{ s}^{-1} \text{ molecule}^{-2} \text{ cm}^6$$

$k_d^\circ$  is the average third-order dimerization rate constant for the considered pyrrolidine-piperidine mixture. Similar dimerization reactions have been shown to follow a rate law consistent with the likely mechanism involving collisional deactivation of the excited dimer initially formed (23, 24):



where  $k = k_t k_s(\text{A})/[k_b + k_s(\text{A})]$ .

This means that these reactions approach second order at high pressure and third order at low pressure.

The preceding results show that the considered dimerization reactions follow third-order kinetics implying rate-limiting collisional deactivation, which is also the case for similar amine systems in the same pressure range (24).

## CONCLUSION

Ion confinement in the rf-only collision cell of a tandem quadrupole mass spectrometer allows the study of a reaction mixture for variable reaction times and thus gives access to reliable kinetic and thermodynamic data for the reactions involved. The described application of this method to quantitatively characterize competitive reactions between pyrrolidine and piperidine in the gas phase demonstrates that it has the potential for investigation of complex reaction mechanisms. Application of the ion confinement technique to various ion-molecule reactions, for instance in the area of gas-phase organometallic chemistry, is thus very promising.

## ACKNOWLEDGMENT

We thank Abdelouahid Dahrouch for his contribution to the most recent experiments, Dr. Nicole Morin for helpful

technical assistance, and Professor J. T. Watson for useful discussions. The efficient technical assistance of the Nermag staff is gratefully acknowledged.

Registry No. Py, 123-75-1; Pi, 110-89-4; PyH, 55526-39-1; PiH, 17523-59-0; NH<sub>4</sub>, 14798-03-9.

#### LITERATURE CITED

- (1) Hartmann, H.; Wanczeck, K. P. *Ion Cyclotron Resonance Spectrometry II*; Lecture Notes in Chemistry 31; Springer-Verlag: Berlin, Heidelberg, New York, 1982.
- (2) Cunningham, A. J.; Payzant, J. D.; Kebarle, P. *J. Am. Chem. Soc.* **1972**, *94*, 7627.
- (3) Kebarle, P. *Annu. Rev. Phys. Chem.* **1977**, *28*, 445.
- (4) Meisels, G. G.; Illies, A. J.; Stradling, R. S.; Jennings, K. R. *J. Chem. Phys.* **1978**, *68*, 866.
- (5) Solomon, J. J.; Field, F. H. *J. Am. Chem. Soc.* **1975**, *97*, 2625.
- (6) Smith, D.; Adams, N. G. In *Gas Phase Ion Chemistry*; Bowers, M. T., Ed.; Academic Press: New York, San Francisco, London, 1979; Vol. 1, p 1.
- (7) Armitage, M. A.; Higgins, M. J.; Lewars, E. G.; March, R. E. *J. Am. Chem. Soc.* **1980**, *102*, 5064.
- (8) Brodbelt-Lustig, J. S.; Cooks, R. G. *Talanta*, in press.
- (9) Doinikowski, G. G.; Kristo, M. J.; Enke, C. G.; Watson, J. T. *Int. J. Mass Spectrom. Ion Processes* **1988**, *82*, 1.
- (10) Beaugrand, C.; Devant, G.; Jaouen, D.; Mestdag, H.; Rolando, C. *Spectrosc. Int. J.* **1987**, *5*, 265.
- (11) Beaugrand, C.; Devant, G.; Jaouen, D.; Rolando, C. *Int. J. Mass Spectrom. Ion Processes*, in press.
- (12) Bowers, M. T.; Aue, D. H.; Webb, H. M. *J. Am. Chem. Soc.* **1971**, *93*, 4314.
- (13) Hiraoka, K.; Takimoto, H.; Yamabe, S. *J. Am. Chem. Soc.* **1987**, *109*, 7346.
- (14) Aue, D. H.; Webb, H. M.; Bowers, M. T. *J. Am. Chem. Soc.* **1976**, *98*, 311.
- (15) Lias, S. G.; Liebman, J. F.; Levin, R. D. *J. Phys. Chem. Ref. Data* **1984**, *13*, 695.
- (16) Davidson, W. A.; Bowers, M. T.; Su, T.; Aue, D. H. *Int. J. Mass Spectrom. Ion Phys.* **1977**, *24*, 83.
- (17) Aue, D. H.; Bowers, M. T. In *Gas Phase Ion Chemistry*; Bowers, M. T., Ed.; Academic Press: New York, San Francisco, London, 1979; Vol. 2, p 1.
- (18) Yamdagni, R.; Kebarle, P. *J. Am. Chem. Soc.* **1973**, *95*, 3504.
- (19) Meot-Ner (Mautner), M. *J. Am. Chem. Soc.* **1984**, *106*, 1257.
- (20) Wren, A. G.; Gilbert, P. T.; Bowers, M. T. *Rev. Sci. Instrum.* **1978**, *49*, 531.
- (21) Scala, A. A.; Caputo, M. G.; Billings, D. J. *Heterocycl. Chem.* **1986**, *23*, 1027.
- (22) Su, T.; Bowers, M. T. In *Gas Phase Ion Chemistry*; Bowers, M. T., Ed.; Academic Press: New York, San Francisco, London, 1979; Vol. 1, p 83 and references cited therein.
- (23) Meot-Ner, M.; Field, F. H. *J. Am. Chem. Soc.* **1975**, *97*, 5339.
- (24) Neilson, P. V.; Bowers, M. T.; Chau, M.; Davidson, W. R.; Aue, D. H. *J. Am. Chem. Soc.* **1978**, *100*, 3649.

RECEIVED for review July 6, 1988. Revised February 24, 1989. Accepted March 16, 1989. The authors are indebted to the Ministère de l'Éducation Nationale (Ecole Normale Supérieure and the grant Action Recherche Universitaire Entreprise) and to the Centre National de la Recherche Scientifique for their financial support of this work.

## Sequence Analysis of Highly Sulfated, Heparin-Derived Oligosaccharides Using Fast Atom Bombardment Mass Spectrometry

Larry M. Mallis\*

High Resolution Mass Spectrometry Facility, The University of Iowa, Iowa City, Iowa 52242

Hui M. Wang, Duraikkannu Loganathan, and Robert J. Linhardt

Division of Medicinal and Natural Products Chemistry, College of Pharmacy, The University of Iowa, Iowa City, Iowa 52242

**Heparin, a polydisperse, sulfated copolymer of 1 → 4 linked glucosamine and uronic acid residues, has been used clinically as an anticoagulant for half a century. Despite a yearly use of over 50 million doses in the U.S. alone, heparin's exact chemical structure remains unclear. The negative ion fast atom bombardment mass spectrometry (FAB-MS) analysis is presented for a series of enzymatically prepared, homogeneous, structurally characterized, highly sulfated, heparin-derived oligosaccharides using triethanolamine as the FAB matrix. In addition to the clear presence of monoanionic sodiated molecular ions, structurally significant (sequence) fragment ions are observed and characterized with respect to the known structure for five of the heparin-derived oligosaccharides. The structure of a sixth oligosaccharide is predicted by using negative ion FAB-MS and subsequently confirmed by chemical, enzymatic, and NMR spectroscopic methods.**

#### INTRODUCTION

Heparin, a polydisperse (having multiple sugar chain lengths), sulfated polysaccharide of 1 → 4 linked glucosamine

and uronic acid residues, has been used clinically as an anticoagulant for half a century (1). Despite a yearly use of over 50 million doses in the U. S. alone (1), the exact chemical structure of heparin remains unclear. The role of heparin in anticoagulation involves the regulation of the coagulation cascade primarily through its potentiation of serine protease inhibitors (2) and is due to the presence of specific protein binding sites in the heparin chain (3, 4). The heparin macromolecule is a proteoglycan (molecular weight approximately 1 000 000 amu) that consists of several polysaccharides having approximate molecular weight of 100 000 amu attached to a protein core (5). Although the structure-activity relationship of the heparin-serine protease inhibitor interaction has been explored in detail (6, 7), considerably less is known about the structural requirements for heparin's other activities (8, 9).

Glycosaminoglycan (GAG)-heparin results from the metabolic processing of proteoglycan heparin by proteases and a β-endoglucuronidase resulting in polydisperse polysaccharide chains of 5000-40000 amu (average of 13 000 amu). The sequence of the polysaccharide chains comprising GAG-heparin is of considerable interest (as this is heparin's drug form); thus heparin lyase is used to enzymatically depolymerize GAG-heparin into smaller oligosaccharides more suitable for structural analysis (10). In general, the structure and sequence of these heparin-derived oligosaccharides have been deter-

\* Author to whom correspondence should be addressed.